CHAPTER 5

EXPERIMENTAL RESULTS ON A THREE-DISK ROTOR

After investigating the effectiveness of an AMD in damping subsynchronous vibrations in a single-disk rotor, the author was encouraged to run some tests in a multi-mass rotor. The three-disk rotor described in Chapter 2 and shown in Figure 5.1 was used to do so. Similar to the experiments carried out on the single-disk rotor, two AMBs offering the capability of being used either to excite the rotor or to perform active control were placed on the rotor. This allowed the evaluation of the effect of the AMD in two locations, at one quarter of the rotor span (AMD-24) and at two thirds of the rotor span (AMD-13), without performing any changes in the configuration of the rotor.

Therefore, two sets of experiments were conducted. In the first set of tests, a sine wave was injected through the AMD-24, while using the AMD-13 to damp the perturbation. In the second group of experiments, the AMD-13 was used to inject a sine wave while the AMD-24 was used to perform active control on the rotor.

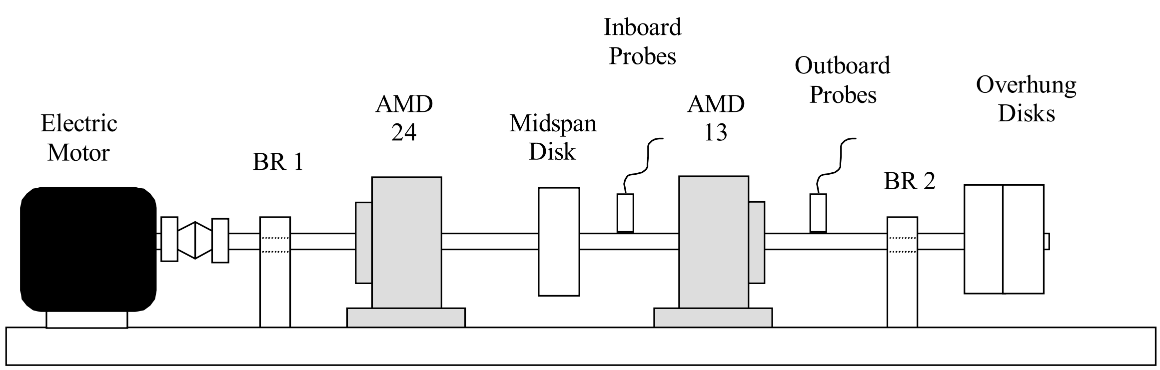

Figure 5.1: Schematic showing the three-disk rotor configuration (not to scale)

The experiments were conducted running the three-disk rotor kit at approximately twice its first critical speed and injecting a sine wave that would approximately excite the first critical speed of the rotor. Due to the difference between the calculated undamped first critical speed, 1529 RPM (25.5 Hz), and the damped measured first critical speed, 1820 RPM (30.3 Hz), an evaluation of the natural frequencies of the rotor while it was not running was performed. Random noise was injected through the AMD-24 and the response to this excitation was measured at one of the probes in order to obtain the frequency response function and determine the natural frequencies. The first natural frequency was located at 1440 RPM (24 Hz). Even though the location of the critical speed varies when the rotor is spinning, the author considered 1440 RPM (24 Hz) as the value to be used in this set of experiments.

5.1 Case 1: Excitation at two thirds of the rotor-span
Damper at quarter-span (AMD-24)

5.1.1 Excitation at ½ X

The rotor was taken up to 2880 RPM (48 Hz), approximately twice the first critical speed of the rotor configuration with the AMDs off and a 0.4 V sine wave at 1440 RPM (24 Hz), simulating a ½ X subsynchronous vibration, was injected through the two-thirds rotor-span AMD (AMD-13) resulting in a 5.2 mils pp vibration at that frequency at the vertical inboard probe. The quarter-span AMD (AMD-24) was subsequently turned on resulting in a reduction of this vibration component to 0.3 mils pp. In addition to the 94% reduction in subsynchronous vibration, the uncompensated synchronous vibration remained essentially unchanged. The amplitude of the direct vibration decreased from 9.3 mils pp to 4.7 mils pp (49%). The spectra of the uncompensated vibration signal at the vertical inboard probe with the AMD-24 "off" and "on" are shown in Figure 5.2 (a) and (b) respectively. Table 5.1 lists the variation in amplitude of the synchronous, subsynchronous and direct vibrations at the four probe locations. After observing the high amplitude of the uncompensated synchronous vibrations, an attempt of balancing the rotor was made but it was not possible to improve the balance of the rotor.

For this case, the stiffness expected for the AMD-24 is 1276 lbf/in at 48 Hz and 1242 lbf/in at 24 Hz. The expected damping for the AMD-24 is 2.95 lb-s/in at 48 Hz and 2.90 lb-s/in at 24 Hz.

In order to address the possibility of shaft bow effects in the increase of the uncompensated synchronous vibration, the 1 X compensated component was examined throughout the operational speed range of the rotor. The rotor kit was then ramped up to 9000 RPM with a perturbation of 0.4 V at 1440 RPM (24 Hz) and with the AMD-24 off. The same test was performed with the AMD-24 on. The effect of the AMD-24 on the compensated synchronous vibration is shown in the Bode plots in Figure 5.3 (a) and (b). Reductions in the compensated synchronous vibration from 8.0 mils pp to 3.0 mils pp (63%) were observed.

This indicates that the ineffectiveness of the AMD-24 in damping the uncompensated synchronous vibration may be due to the large shaft bow. This effect is eliminated when the synchronous vibration is compensated with respect to the slow roll vector.

Table 5.1: Effect of the AMD-24 on the direct, synchronous and subsynchronous amplitudes of the three-disk rotor at 2880 RPM (48 Hz) with a perturbation of 0.4 V at 1440 RPM (24 Hz), ½ X the rotational speed, through the AMD-13

Probe Location	**AMD-24 "Off"**			**AMD-24 "On"**			**Variation in Amplitude**		
	Direct Amplitude mils pp	Synchronous Amplitude mils pp	Subsynchronous Amplitude mils pp	Direct Amplitude mils pp	Synchronous Amplitude mils pp	Subsynchronous Amplitude mils pp	Direct Amplitude %	Synchronous Amplitude %	Subsynchronous Amplitude %
Inboard vertical	9.3	4.6	5.2	4.7	4.5	0.3	- 49	- 2	- 94
Inboard horizontal	5.9	3.3	4.1	4.0	3.8	0.2	- 32	+15	- 95
Outboard vertical	2.6	1.0	1.5	1.4	1.3	0.1	- 46	+30	- 93
Outboard horizontal	1.1	0.6	0.6	0.7	0.6	0	- 36	0	- 100

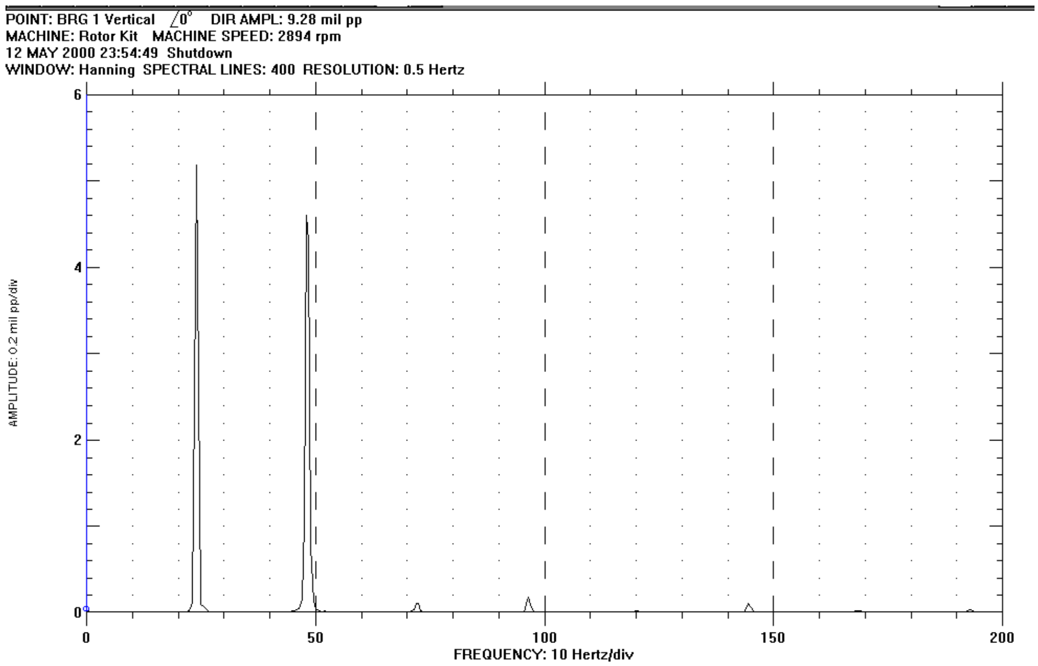

(a)

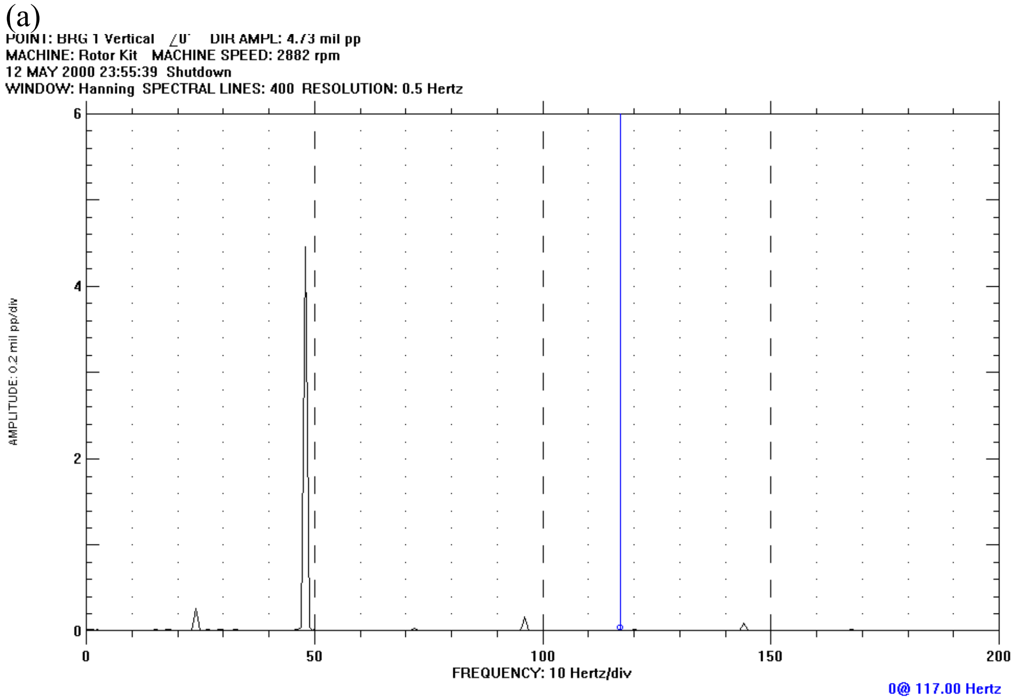

(b)

Figure 5.2: Spectrum of the vibration signal at the vertical inboard probe, three-disk rotor at 2880 RPM (48 Hz) and a perturbation at 24 Hz through AMD-13. (a) AMD-24 off. (b) AMD-24 on.

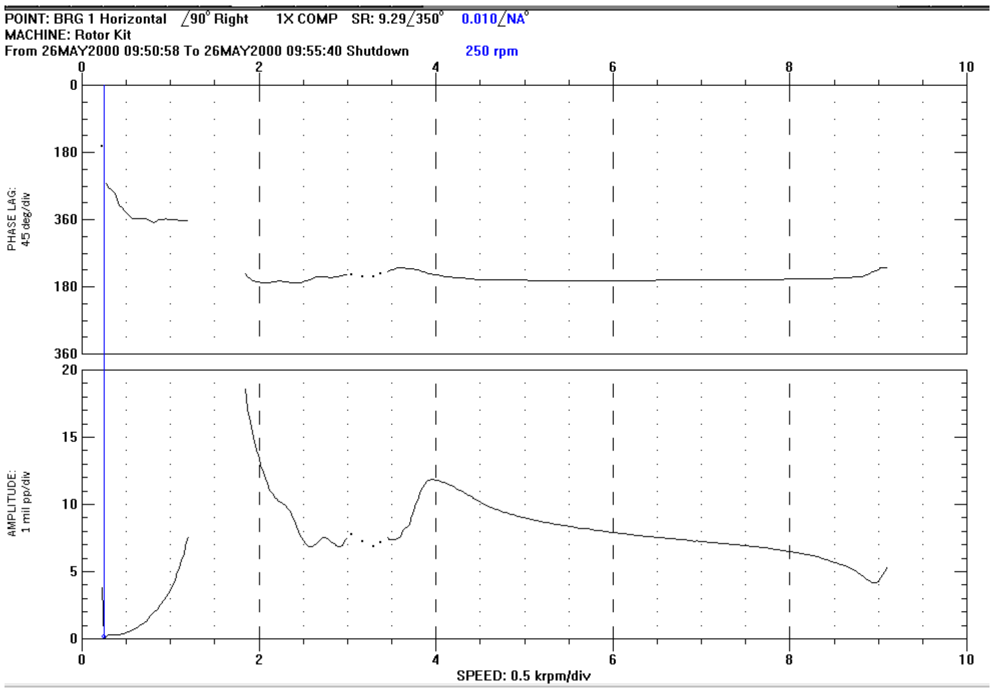

(a)

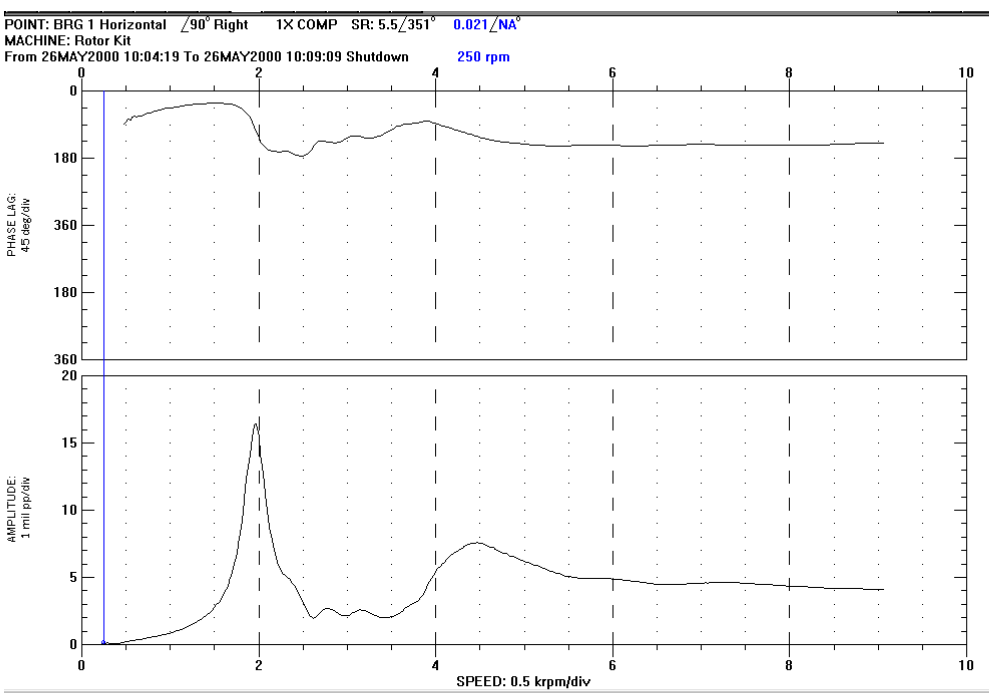

(b)

Figure 5.3: Bode plots of the three-disk rotor with an excitation of 0.4 V at 24 Hz through the AMD-13. (a) AMD-24 off. (b) AMD-24 on.

5.2 Case 2: Excitation at quarter-span

Damper at two-thirds rotor-span (AMD-13)

5.2.1 Excitation at ½ X, K_{AMD-13}=1276 lbf/in

In this test, the rotor was taken up to 2880 RPM (48.0 Hz), twice the first critical speed of the rotor configuration with the AMDs off and a 0.4 V sine wave at 1440 RPM (24.0 Hz) was injected through the quarter-span AMD (AMD-24) resulting in a 5.1 mils pp vibration at this frequency at the vertical inboard probe. The two thirds rotor-span AMD (AMD-13) was subsequently turned on resulting in a reduction of this vibration component to 0.1 mils pp. In addition to the 98% reduction in subsynchronous vibration, a reduction of 18% of the uncompensated synchronous vibration was also achieved. The amplitude of the direct vibration decreased in 37 %, from 8.1 mils pp to 5.1 mils pp. The spectra of the uncompensated vibration signal at the vertical inboard probe with the AMD-13 "off" and "on" are shown in Figure 5.4 (a) and (b), respectively. The variations in amplitude of the synchronous, subsynchronous and direct vibrations at the four probe locations are listed in Table 5.2. For this case, the stiffness expected for the AMD-24 is 1276 lbf/in at 48 Hz and 1242 lbf/in at 24 Hz. The expected damping for the AMD-24 is 2.95 lb-s/in at 48 Hz and 2.90 lb-s/in at 24 Hz.

In order to address the possibility of shaft bow effects in the low effect of the AMD in decreasing the uncompensated synchronous vibration, the 1 X compensated component was examined throughout the operational speed range of the rotor. The rotor kit was then ramped up to 9000 RPM with a perturbation of 0.4 V at 1440 RPM (24 Hz) with the AMD-13 off. The same test was performed with the AMD-13 on. The effect of the AMD-13 on the compensated synchronous vibration is shown in the Bode plots in Figure 5.5 (a) and (b). Reductions in the compensated synchronous vibration from 7.0 mils pp to 3.0 mils pp (57%) were observed. This indicates that the ineffectiveness of the AMD-24 in damping the uncompensated synchronous vibration may be due to the large shaft bow. This effect is eliminated when the synchronous vibration is compensated with respect to the slow roll vector.

5.2.2 Excitation at ½ X, K_{AMD-24}=0 lbf/in

In this test, the rotor was taken up to 2880 RPM (48.0 Hz), twice the first critical speed of the rotor configuration with the AMDs off and a 0.4 V sine wave at 1440 RPM (24.0 Hz) was injected through the quarter-span AMD (AMD-24) resulting in a 2.8 mils pp vibration at this frequency at the vertical inboard probe. The two thirds rotor-span AMD (AMD-13) was subsequently turned on resulting in a reduction of this vibration component from 2.8 mils pp to 0.2 mils pp. In addition to the 93% reduction in subsynchronous vibration, a reduction of 17% of the uncompensated synchronous vibration was also achieved. The amplitude of the direct vibration decreased in 33 %, from 7.3 mils pp to 4.9 mils pp. The spectra of the uncompensated vibration signal at the vertical inboard probe with the AMD-13 "off" and "on" are shown in Figure 5.6 (a) and (b), respectively. The variations in amplitude of the synchronous, subsynchronous and direct vibrations at the four probe locations are listed in table 5.3.

For this case, the stiffness expected for the AMD-24 is 0 lbf/in at 48 Hz and 24 Hz. The expected damping for the AMD-24 is 3.18 lb-s/in at 48 Hz and 3.13 lb-s/in at 24 Hz.

Even though a Bode plot of the compensated synchronous vibration was not obtained for this case, it is also expected that the ineffectiveness of the AMD-24 in damping the uncompensated synchronous vibration may be due to the large shaft bow.

Table 5.2: Effect of the AMD-13 on the direct, synchronous and subsynchronous amplitudes of the three-disk rotor at 2880 RPM (48 Hz) with a perturbation of 0.4 V at 24 Hz, 1/2 X the rotational speed, through the AMD-24 K_{AMD-24}=1276 lbf/in

Probe Location	**AMD-13 “Off”**			**AMD-13 “On”**			**Variation in Amplitude**		
	Direct Amplitude mils pp	Synchronous Amplitude mils pp	Subsynchronous Amplitude mils pp	Direct Amplitude mils pp	Synchronous Amplitude mils pp	Subsynchronous Amplitude mils pp	Direct Amplitude %	Synchronous Amplitude %	Subsynchronous Amplitude %
Inboard vertical	8.1	5.1	5.1	5.1	4.2	0.1	- 37	- 18	- 98
Inboard horizontal	5.5	3.7	4.3	4.8	4.0	0.1	- 13	+ 8	- 98
Outboard vertical	2.1	1.1	1.5	0.8	0.7	0	- 62	- 36	- 100
Outboard horizontal	1.1	0.7	0.7	0.5	0.4	0	- 55	- 43	- 100

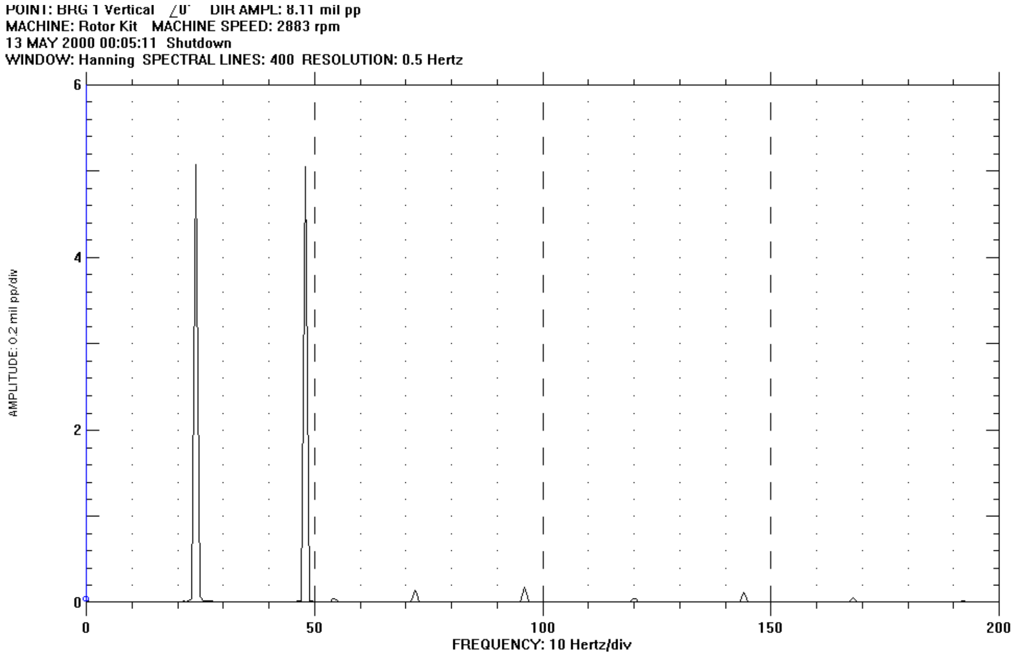

(a)

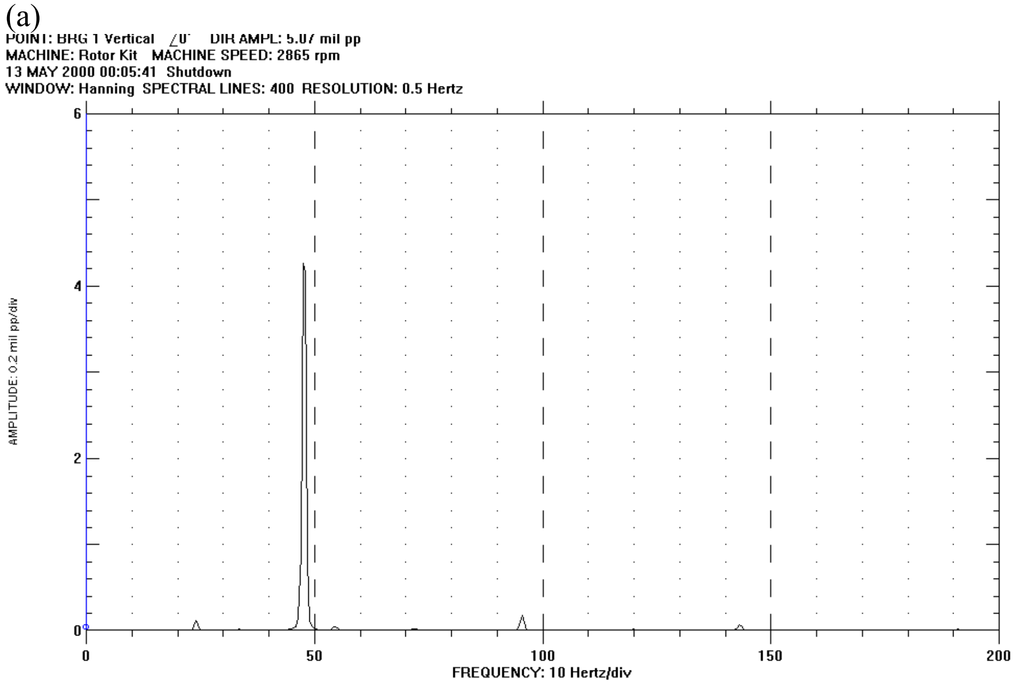

(b)

Figure 5.4: Spectrum of the vibration signal at the vertical inboard probe, three-disk rotor at 2880 RPM (48 Hz) and a perturbation at 24 Hz through AMD-24. K_{AMD-24}=1276 lbf/in. (a) AMD-13 off. (b) AMD-13 on.

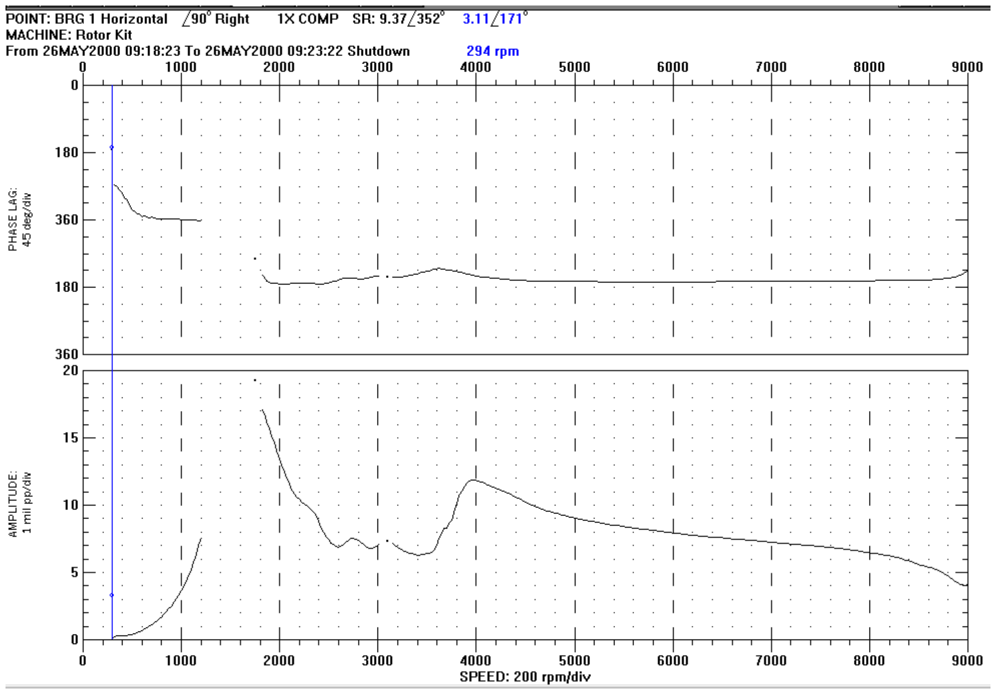

(a)

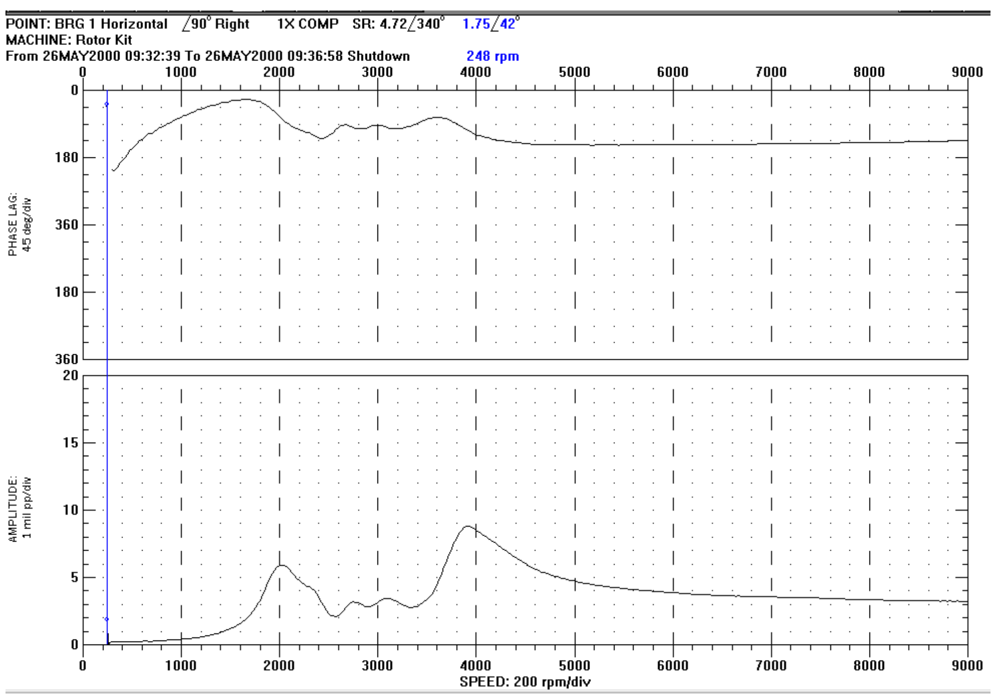

(b)

Figure 5.5: Bode plots of the three-disk rotor with an excitation of 0.4 V at 24 Hz through the AMD-24. (a) AMD-13 off. (b) AMD-13 on.

Table 5.3: Effect of the AMD-13 on the direct, synchronous and subsynchronous amplitudes of the three-disk rotor at 2880 RPM (48 Hz) with a perturbation of 0.4 V at 1440 RPM (24 Hz), ½ X the rotational speed, through the AMD-24 K_{AMD-24}=0 lbf/in

Probe Location	**AMD-13 "Off"**			**AMD-13 "On"**			**Variation in Amplitude**		
	Direct Amplitude mils pp	Synchronous Amplitude mils pp	Subsynchronous Amplitude mils pp	Direct Amplitude mils pp	Synchronous Amplitude mils pp	Subsynchronous Amplitude mils pp	Direct Amplitude %	Synchronous Amplitude %	Subsynchronous Amplitude %
Inboard vertical	7.3	5.3	2.8	4.9	4.4	0.2	- 33	- 17	- 93
Inboard horizontal	5.5	3.8	2.1	3.6	3.3	0.1	- 35	- 13	- 95
Outboard vertical	1.6	1.0	0.7	1.0	0.8	0.1	- 60	- 20	- 85
Outboard horizontal	0.9	0.6	0.3	0.6	0.4	0	- 33	- 33	- 100

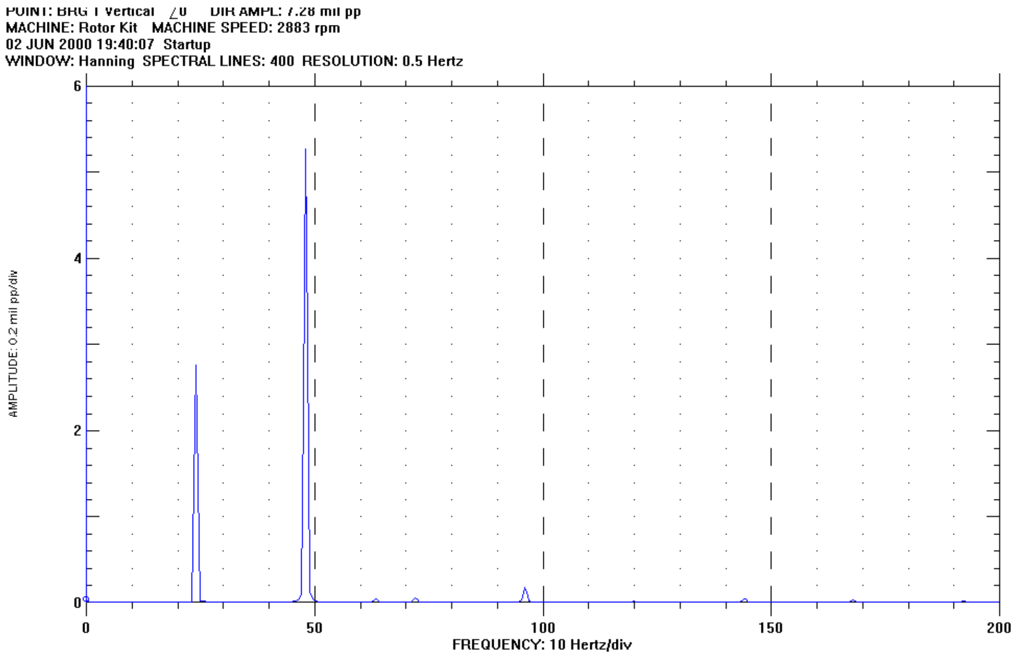

(a)

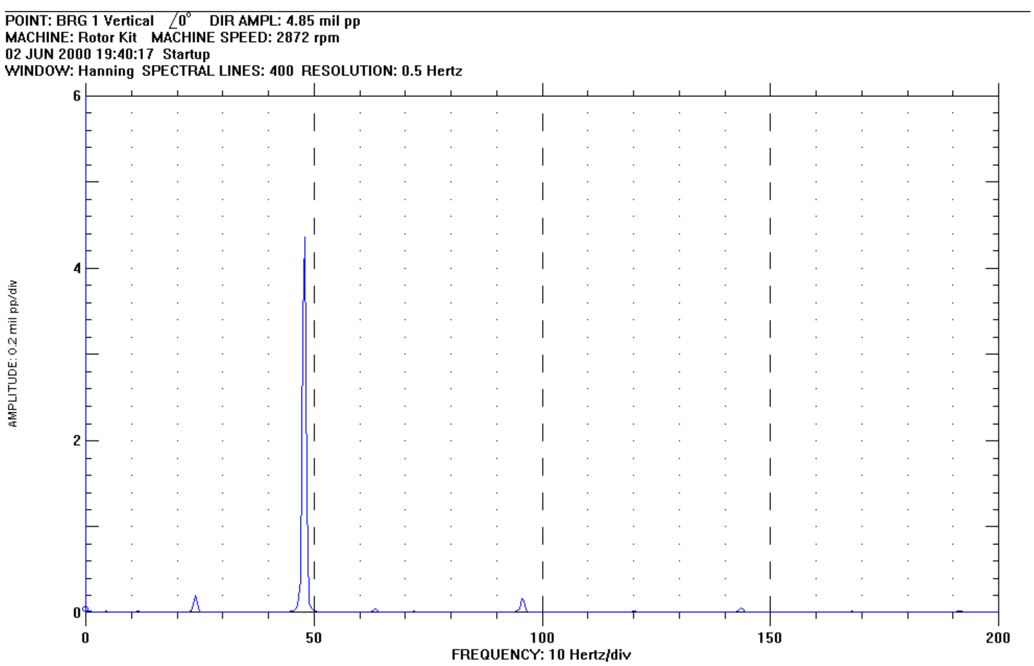

(b)

Figure 5.6: Spectrum of the vibration signal at the vertical inboard probe, three-disk rotor at 2880 RPM (48 Hz) and a perturbation at 24 Hz through AMD-24. $K_{AMD\text{-}24}$=0 lbf/in. (a) AMD-13 off. (b) AMD-13 on.